

Article

Future Changes in Tropical Cyclone and Easterly Wave Characteristics over Tropical North America

Christian Dominguez ^{1,*} , James M. Done ²  and Cindy L. Bruyère ^{2,3} 

¹ Centro de Ciencias de la Atmósfera, Universidad Nacional Autónoma de México (UNAM), Mexico City 04510, Mexico

² National Center for Atmospheric Research, Boulder, CO 80301, USA; done@ucar.edu (J.M.D.); bruyerec@ucar.edu (C.L.B.)

³ Environmental Sciences and Management, North-West University, Potchefstroom 2531, South Africa

* Correspondence: dosach@atmosfera.unam.mx

Abstract: Tropical Cyclones (TCs) and Easterly Waves (EWs) are the most important phenomena in Tropical North America. Thus, examining their future changes is crucial for adaptation and mitigation strategies. The Community Earth System Model drove a three-member regional model multi-physics ensemble under the Representative Concentration Pathways 8.5 emission scenario for creating four future scenarios (2020–2030, 2030–2040, 2050–2060, 2080–2090). These future climate runs were analyzed to determine changes in EW and TC features: rainfall, track density, contribution to seasonal rainfall, and tropical cyclogenesis. Our study reveals that a mean increase of at least 40% in the mean annual TC precipitation is projected over northern Mexico and southwestern USA. Slight positive changes in EW track density are projected southwards 10° N over the North Atlantic Ocean for the 2050–2060 and 2080–2090 periods. Over the Eastern Pacific Ocean, a mean increment in the EW activity is projected westwards across the future decades. Furthermore, a mean reduction by up to 60% of EW rainfall, mainly over the Caribbean region, Gulf of Mexico, and central-southern Mexico, is projected for the future decades. Tropical cyclogenesis over both basins slightly changes in future scenarios (not significant). We concluded that these variations could have significant impacts on regional precipitation.

Keywords: tropical cyclones; easterly waves; future changes in rainfall; changes in tropical cyclogenesis



Citation: Dominguez, C.; Done, J.M.; Bruyère, C.L. Future Changes in Tropical Cyclone and Easterly Wave Characteristics over Tropical North America. *Oceans* **2021**, *2*, 429–447. <https://doi.org/10.3390/oceans2020024>

Academic Editor: Hiroyuki Murakami

Received: 14 April 2021

Accepted: 7 June 2021

Published: 10 June 2021

Publisher's Note: MDPI stays neutral with regard to jurisdictional claims in published maps and institutional affiliations.



Copyright: © 2021 by the authors. Licensee MDPI, Basel, Switzerland. This article is an open access article distributed under the terms and conditions of the Creative Commons Attribution (CC BY) license (<https://creativecommons.org/licenses/by/4.0/>).

1. Introduction

Tropical Cyclones (TCs) are widely known worldwide for their destructive effects on the continental landmass and the high economic losses associated with their passages [1]. For instance, TCs are linked with 86.5% of the annual disaster costs in Mexico, where the main hazard is the heavy rainfall they produced [2]. Dominguez et al. [3] show that disaster costs in Mexico remarkably depend on natural variability, such as ENSO, because the national social vulnerability is high. Tropical storms or even tropical depressions can produce such huge amounts of rainfall that one single event can increase the chances of disaster occurrence. However, TCs also play an important role as moisture carriers for arid and semiarid regions, where they can contribute up to 30% of the accumulated seasonal rainfall and help to ameliorate water scarcity [4]. In that sense, exploring future regional changes in TC features (e.g., rainfall and frequency) is considered necessary for water availability projections and domestic decision makers.

Future scenarios for tropical cyclone activity reveal different results that depend on the basin, model configuration, representation of ocean-air feedback, periods of study, and the Representative Concentration Pathways (RCPs) that were considered, among others [5–8]. For example, Bacmeister et al. [9] and Wehner et al. [10] explored high-resolution simulations from the Community Atmosphere Model and found that while

high-resolution models do not largely improve simulated climate, interannual variability of TCs is better simulated. Recently, Bacmeister et al. [11] used the Community Earth System Model (CESM) at a 28 km spatial resolution and determined that TC activity globally decreases in the RCP4.5 and RCP8.5 future scenarios. Apart from that, the High Resolution Model Intercomparison Project (HighResMIP v1.0) was created in 2016 as a coordinated effort among several international centers to investigate the impact of increased horizontal resolution based on multimodel ensembles and is part of the Coupled Model Intercomparison Experiment Phase 6 (CMIP6) [12]. The main goal of HighResMIP v1.0 is to determine the dynamical and physical mechanisms that lead to differences in model simulations, which, in the end, will foster confidence in model skill or help to understand model constraints [12].

As part of HighResMIP v1.0, Bao et al. [13] recently experimented with increasing horizontal resolution from 1.0° to 0.25° on one General Climate Model (GCM), called CAS FGOALS-f3-H, in 2020. It was found that this model produced more long-lived TCs in all basins from 2001–2010, when compared with 1.0° spatial resolution simulations. Additionally, Roberts et al. [14,15] explored the future TC activity in a high-resolution multimodel ensemble from HighResMIP. It is important to mention that these studies are among the first to use high-resolution GCMs to analyze future changes in TCs. They found that an increase in the model's spatial resolution leads to a decrease in negative density bias, mainly over the North Atlantic (NATL) and Eastern Pacific (EPAC) Oceans. These results also show that TC activity over the NATL will decrease, and tracks over EPAC will experience a poleward shift in the future (2020–2050).

Interestingly, Knutson et al. [16] previously found similar results over NATL using a regional climate model (RCM) based on CMIP3 and CMIP5 scenarios: a decrease ($\sim 20\%$) in TC frequency, similar to the results found by Roberts et al. [14], and an increase ($\sim 60\%$ on average) in TC intensity. However, the results for future TC activity over EPAC are inconsistent. While GCMs from CMIP5 show a reduction in frequency, RCM outputs point out an increase over this basin [8]. In terms of rainfall, Knutson et al. [17,18] analyzed some studies that explored rainfall-rate change for NATL and EPAC and determined that TC rainfall will increase $\sim 5\text{--}25\%$ in both basins by the end of the century. The latter results from an increase in the large-scale atmospheric water vapor content, tropospheric and oceanic warming.

It is worth mentioning that until now, several research questions regarding changes in features of tropical phenomena (i.e., TC precipitation or tropical-wave-related rainfall) have been only addressed by the RCM experiments, focusing on specific basins. Although HighResMIP can provide valuable information about future changes in TCs due to the high spatial resolution, it would be ideal to compare the high-resolution GCM outputs with RCM simulations. In this sense, this comparison will let us understand to what extent RCMs can still produce advantageous projections of changes in tropical phenomena. This information could inform future tasks of the Coordinated Regional Climate Downscaling Experiment, known as CORDEX.

Easterly Waves (EWs), commonly known as tropical-depression-type waves, are Rossby wave-like disturbances over the tropics that can be precursors of TCs [19]. These waves propagate westwards and last up to 6 days over NATL [20] and up to 8 days over EPAC [21]. Over the NATL basin, two waveguides can be distinguished: one to the south of 10° N (hereafter southern waveguide) and the other to the north, around 15° N (hereafter northern waveguide); each playing different roles in tropical cyclogenesis [22]. Overall, it has been found that $\sim 50\%$ and $\sim 70\%$ of TCs from NATL and EPAC originate from EWs, respectively [23–25]. Apart from being important for tropical cyclogenesis, EWs are also relevant moisture carriers for the tropics because they can contribute up to 60% of seasonal accumulated rainfall over Tropical North America (TNA) [25]. However, this role has been less explored than the heavy rainfall produced by TCs.

Moreover, most EW studies have focused on exploring the relationship between EWs and the West Africa monsoon [26,27]. For example, Martin and Thorncroft [28] found

that CMIP5 models have problems capturing EW propagation, maintenance, and growth mechanisms over the west African coast and concluded that high-resolution models can better represent EW dynamics. Furthermore, Kebe et al. [29] explained that a projected reduction in the EW activity impacts the seasonal summer precipitation over West Africa for the 2080–2099 period. However, future changes in EW rainfall over the TNA remain unexplored. Consequently, no studies investigate how EW rainfall over TNA will change in the future under climate change conditions. Having this information is crucial for local stakeholders and farmers that will struggle with climate-change effects.

The main objective of this study is to explore future changes in the rainfall produced by TCs and EWs over TNA using a regional climate simulation ensemble under a future climate scenario. Our emphasis is on analyzing the response of the tropical phenomena characteristics to different representations of large-scale forcing rather than investigating the full set of possible future scenarios. In this sense, our three-member ensemble forced by only one GCM does not sample the full range of future possibilities due to different emission scenarios, internal GCM variability, or diverse ocean responses to radiative forcing. This study investigates potential changes in tropical cyclogenesis, TC rainfall, and EW rainfall, as well as their contribution to summer rainfall (defined here as accumulated precipitation from May to November) of the current climate represented by the 1990–2000 decade, along with two near future decades (2020–2030, 2030–2040) and two far future decades (2050–2060, 2080–2090), by using a three-member ensemble. The results of this study can be relevant for regional climate change adaptation strategies in most countries from Latin America. We use dynamical downscaling to provide detailed information about TC and EW characteristics that coarse spatial resolution GCMs could miss (e.g., structure, evolution, and their impact on regional climate). An RCM grid spacing of 36 km has been demonstrated to represent adequately tropical synoptic circulations and features [7]. Some studies show that RCMs realistically captured spatial distribution, evolution, generation, and organized convection of EWs [30,31]. The latter indicates that RCMs can provide valuable regional information about TC and EW frequency changes and their associated rainfall.

The next section describes the reanalysis data and observed tracks for TCs over NATL and EPAC. The method used to attribute rainfall to TCs and EWs, regional climate model configuration, and criteria for tracking tropical phenomena in the RCM outputs are also discussed. Section 3 analyzes the future changes in seasonal rainfall produced by EWs and TCs over TNA. Future changes in the rate of TCs that originate from EWs are also presented. Finally, the summary and conclusions are given in Section 4.

2. Data and Methods

2.1. Reanalysis, TC Tracks, and Tropical Rainfall Attribution

ERAInterim (ERA-I) is available from 1979 to 2019 and has a T255 spectral resolution (~80 km) on 60 vertical model levels [32]. TC rainfall was defined using the precipitation from this dataset for the 1990–2000 period. TC tracks whose category is a tropical depression, tropical storm, or hurricane over the NATL and EPAC were obtained from the Hurricane Database, also known as HURDAT, for the same period [33]. Following previous studies [4,34,35], TC-related rainfall is defined as the precipitation inside a 500 km radius of influence from the TC center location provided by HURDAT. This approximation has been widely recognized to compute adequately the rainfall associated with TC passages. We compared the TC rainfall obtained from ERA-I with the TC rainfall in the RCM outputs for the 1990–2000 period to determine if regional variations are well captured.

2.2. Regional Climate Model Configuration

One of the advantages of using RCMs is that tropical phenomena, such as TCs and EWs, are better resolved in RCMs than in GCMs, due to their relatively coarser resolution. For this study, we use an existing RCM ensemble described by Bruyère et al. [7]. ERA-I reanalysis drove the Weather Research and Forecasting model version 3.4 (hereafter

WRF; [36]) for producing the current climate simulations (1990–2000). The RCM ensemble was forced by using the Reynolds optimum interpolated analysis [37]. The experiments were designed at the National Center for Atmospheric Research (NCAR) in 2013 and have been used in various studies in the American continent. The domain of the experiments ranges from Canada to Brazil and from Hawaii to the mid-Atlantic Ocean (Figure 1). The domain size is enough for capturing EWs that enter the eastern boundary, whose lateral boundary conditions are provided by the ERAI reanalysis for the current climate runs and by the CESM for future climate runs. These EWs become TCs over the NATL within the RCM domain [7]. Furthermore, the fact that the domain boundaries are far away from TNA's continental landmasses lets the regional climate phenomena evolve freely within the WRF domain, as they are not limited by the boundaries [38].

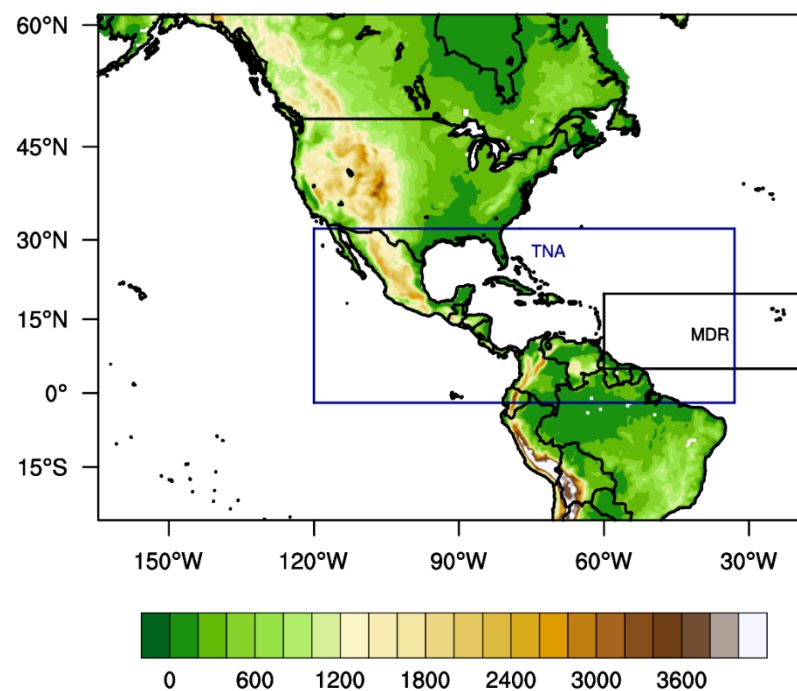


Figure 1. Regional climate model domain. Model terrain height (m) and the two study regions: Tropical North America (TNA) and Main Development Region (MDR).

Three members were chosen from a 24-member model physics ensemble because they performed an adequate simulation of TC activity for the 1990–2000 period, as described in Bruyère et al. [7], and were run at 36 km spatial resolution. The three members have different physical parameterization schemes: radiation scheme (RRTMG [39]); cumulus convection (Kain Fritsch [40], New Simplified Arakawa–Schubert [41], and Tiedtke [42]); microphysics (Thompson [43]) and planetary boundary layer (PBL) (Mellor–Yamada–Janjić [44], and Yonsei University [45]). The Noah scheme [46] was the only land surface scheme used for the experiments. The three members are listed in Table 1. The four letters assigned to the three members represent a combination of parameterizations. For example, the member *rtty* means that RRTMG is the radiation scheme, Tiedtke is the cumulus parameterization, Thompson is the microphysics scheme, and the fourth letter represents the Mellor–Yamada–Janjić planetary boundary layer scheme.

Table 1. The physics combinations of the three members used for the future runs. These members use the same radiation (RRTMG) and microphysics (Thompson) scheme. All simulations are conducted at a 36 km grid spacing.

Cumulus Convection	Planet Boundary Layer	
	<i>Mellor–Yamada–Janjić (M)</i>	<i>Yonsei University (Y)</i>
<i>Kain Fritsch (K)</i>	RKTM	
<i>New Simplified Arakawa–Schubert (N)</i>		RNTY
<i>Tiedtke (T)</i>		RTTY

In this way, we provide robustness of the physical processes to different representations of atmospheric processes. Future climate runs are designed to provide enough samples of different atmospheric representations. The CESM [47], which is part of the CMIP5 [48], drove the future runs under the RCP8.5 future emission scenario [49]. Biases from this global model were removed before forcing the WRF model, following Bruyère et al. [50].

2.3. Criteria for Tracking Tropical Cyclones and Easterly Waves in Model Outputs

2.3.1. Criteria for Tropical Cyclones and Attribution of Rainfall

TCs were tracked using the algorithm created by Hodges [51] in the current and future climate runs. The TRACK technique follows vorticity centers at 700 mb and only retained vortices that have these TC characteristics:

1. The sum of the horizontal temperature difference between the storm and its surroundings at 700 mb, 500 mb, and 300 mb is greater than 2 K.
2. The mean 850 mb wind speed is greater than the mean 300 mb wind speed.
3. The 300 mb horizontal temperature difference between the storm and its surroundings is greater than that at 850 mb.
4. The genesis location must be south of 40° N.
5. The vorticity centers should retain tropical storm wind intensity for a minimum of 36 h.
6. A threshold of wind speed at 10 m should be met: 12 m/s was for all KF simulations and 10 m/s for all other simulations [7].

Specifically, the wind criteria were created following the wind profile method proposed by Walsh (2007) [52]. These six criteria have been demonstrated to adequately work in WRF simulations at 36 km resolution [38]. The TC-related rainfall was also defined as the 500 km radius of influence from the TC-like vortex center location.

2.3.2. Criteria for Easterly Waves and Attribution of Rainfall

EWs were also tracked at 700 mb using the Hodges algorithm, but with different criteria:

1. Westward movement;
2. A lifetime of at least 2 days;
3. The first detected points are over the oceanic domain 5–20° N;
4. Vorticity centers are $1.8 \times 10^{-5} \text{ s}^{-1}$ or greater;
5. Systems travel at least 1000 km;
6. Wind speed at 10 m should be less than 12 m/s for all KF simulations and should be less than 10 m/s for all other simulations.

These objective criteria have been widely used in several studies [20,25,53] and have proved to detect EW frequency adequately. Thus, TCs and EWs are both tracked using the described objective algorithm. EWs and TCs were matched by determining points where EW characteristics are accomplished, and then EWs evolve to meet TC features during the track. In that way, the portion of TCs that come from EWs was obtained for each member.

The EW-related rainfall was defined following previous studies [23,25], where a $15^\circ \times 15^\circ$ region around the center provided by the TRACK technique is used to define precipitation produced by EWs. It is worth mentioning that we suppose that precipitation matches with the positive phase of EWs and that the precipitation is only constrained to the $15^\circ \times 15^\circ$ box. Our approach for considering only the positive phase (represented by positive vorticity) may result in underestimating the rainfall because the negative phase of EWs can still produce shallow convection [27]. This assumption may represent a limitation, and it is discussed in Section 4.

2.3.3. The Kolmogorov–Smirnov Two-Sample Test

We used the Kolmogorov–Smirnov two-sample test (KST) to evaluate if the current and future climate results belong to the same distribution (null hypothesis) [54]. If the null hypothesis cannot be rejected, the current and future runs belong to the same distribution, showing no future shifts in climate. In other words, we assume that radiative forcing of 8.5 W/m^2 associated with an increase in Greenhouse Gas concentration will not uniformly cause changes in future climate for all regions from TNA. All future changes are evaluated at a 95% significance level.

3. Results

3.1. Future Changes in Sea Surface Temperatures and Tropical Precipitation

The CESM provided the sea surface temperatures (SSTs) used to force the three-member ensemble for the four future decades. Mean SST anomalies are defined as the annual mean SST values for four future decades minus the SSTs obtained from the Reynolds optimum interpolated analysis during the 1990–2000 period (Figure 2). The mean SST anomalies are generally projected to increase across the future decades. In the two near-future decades, SST anomalies are shown to rise up to 1.2 K. By the 2050–2060 period, a tropical SST warming is projected to strengthen up to 1.8 K in most regions over the TNA. Notably, the most extreme changes in SSTs will occur in the Gulf of Mexico, part of the Caribbean region, and the belt of $5\text{--}15^\circ \text{ N}$ over EPAC, where SST anomalies vary from 2.4 K to 3 K, for the 2080–2090 period, under the RCP8.5 future emission scenario (Figure 2). However, this uniform increment in SSTs shown in Figure 2 does not mean a uniform increase in tropical convection activity in general [55].

Apart from that, several studies that only focus on TCs have revealed an increase in TC intensity [18,56,57] and TC-related rainfall [16,58] due to changes in SSTs. In particular, Knutson et al. [18] summarized the key findings of global research about the influence of climate change on TCs. They mentioned that changes in tropical tropospheric temperature and SSTs could influence TC activity. Interestingly, TC rainfall rates were determined to increase globally by about 14% for a 2° C warming at medium-to-high confidence, being slightly lower for individual basins.

Bruyère et al. [7] estimate that the three members have adequate skill to simulate precipitation and temperature over Mexico and Central America. However, these members also have a dry/wet bias ($\pm 6 \text{ mm/day}$) and a cold/hot bias ($\pm 4^\circ \text{ C/day}$) for the June–July–August months when compared to the Climate Forecast System Reanalysis (CFSR) during the 1990–2000 period [59]. The member rnty was the best one at simulating the rainfall over TNA. Bruyère et al. [7] also show that tropical rainfall is projected to decrease in regions where the average maximum temperature will increase (i.e., central-southern Mexico and Central America) for the June–July–August months during the far future decades (2050–2060 and 2080–2090). On the contrary, their results indicate a rise in tropical rainfall in some parts of the tropical Pacific Ocean for the four future decades.

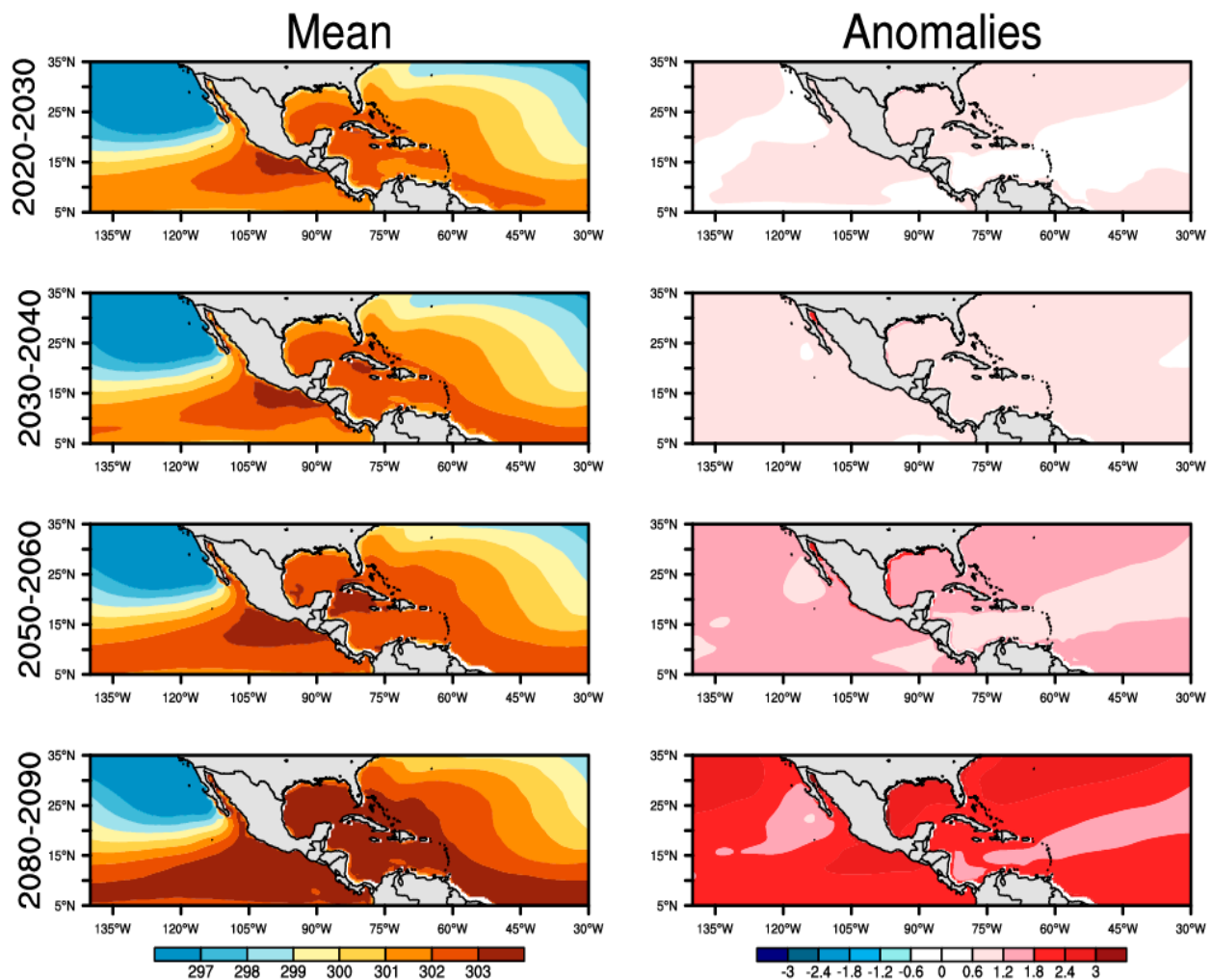


Figure 2. Annual mean (K degrees) and mean anomalies (K degrees) of sea surface temperatures over Tropical North America with respect to the reference period (1990–2000).

In terms of percent change, the three members agree with an increase by up to 50% in the summer rainfall over northern Mexico across the four future decades at a 95% significance level (Figure 3). On the other hand, a decrease of up to 40% in summer rainfall is projected for Central America, northern South America, and the Caribbean region, the changes being more uncertain for the latter region (Figure 3). These results are also consistent with Durán-Quesada et al. [60], who used an ensemble of four GCMs under the RCP2.6, RCP7.0, and RCP8.5 future emission scenarios. Our results suggest that Central America, the Caribbean region, and northern South America will experience droughts in the future, causing water scarcity and impacts in tropical ecosystems [61]. Apart from that, it is notable that non-significant regions increase their area over Central America during the two far future decades, pointing out that uncertainty grows for distant futures.

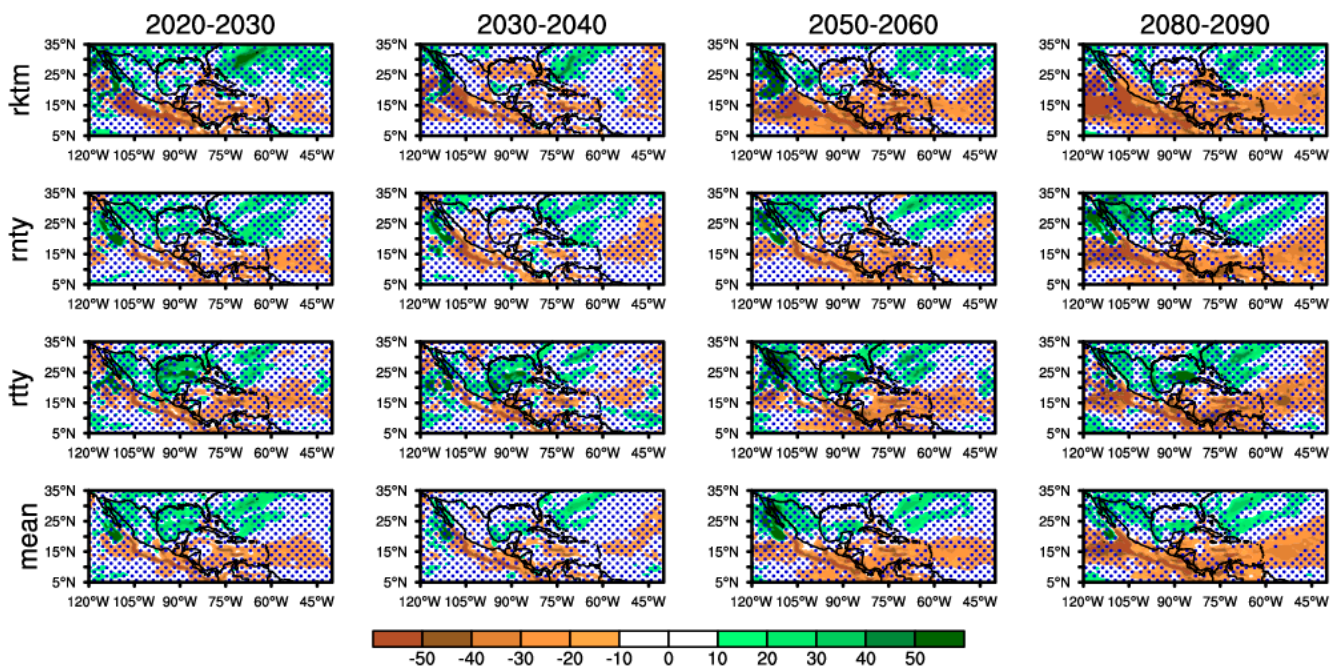


Figure 3. Mean annual percent change (%) in accumulated precipitation from May to November, defined as summer rainfall, with respect to the reference period (1990–2000). The dotted regions indicate a 95% significance level applying the Kolmogorov–Smirnov two-sample test.

3.2. Changes in Tropical Cyclones Features: Rainfall and Track Density

Bruyère et al. [7] show that the cumulus and boundary layer parameterizations have the largest impacts on the annual TC frequency over NATL and EPAC. The observed record of TC activity was 10 ± 3 TCs per year over NATL and 16 ± 4 TCs per year over EPAC. The physical combination of Kain–Fritsch with Mellor–Yamada–Janjić “rktm” registered 12 (17) TCs per year over NATL (EPAC). The combination of Tiedtke with Yonsei University “rtty” produced 8 (14) TCs per year over NATL (EPAC). However, the combination New Simplified Arakawa Schubert/Yonsei University “rnty” generated 9 (6) TCs per year over NATL (EPAC), showing fewer TCs than the observed number over EPAC. In general, TC variability over NATL was successfully captured by the three members during the current climate runs (1990–2000). For the EPAC, only rktm and rnty were able to simulate TC numbers inside the range of one standard deviation.

Mean annual TC track density was computed as the number of tracks per unit area ($1^\circ \times 1^\circ$), and per year from May to November for the three ensemble members (Figure 4a,c,e), the ensemble mean (Figure 4g), and HURDAT tracks (Figure 4i) for the current climate runs. In general, TC track density is successfully represented by the three ensemble members over NATL. However, the spatial distribution of TC tracks is overestimated over EPAC in the belt of 10–15° N by the members rktm and rnty (Figure 4a,e) when compared to HURDAT (Figure 4i). On the contrary, the member rnty underestimates the mean annual TC track density (Figure 4c), as shown by Bruyère et al. [7]. Interestingly, the ensemble mean adequately represents the observed TC track density over EPAC (Figure 4g), although it slightly overestimates TC density near the Western Central America coast.

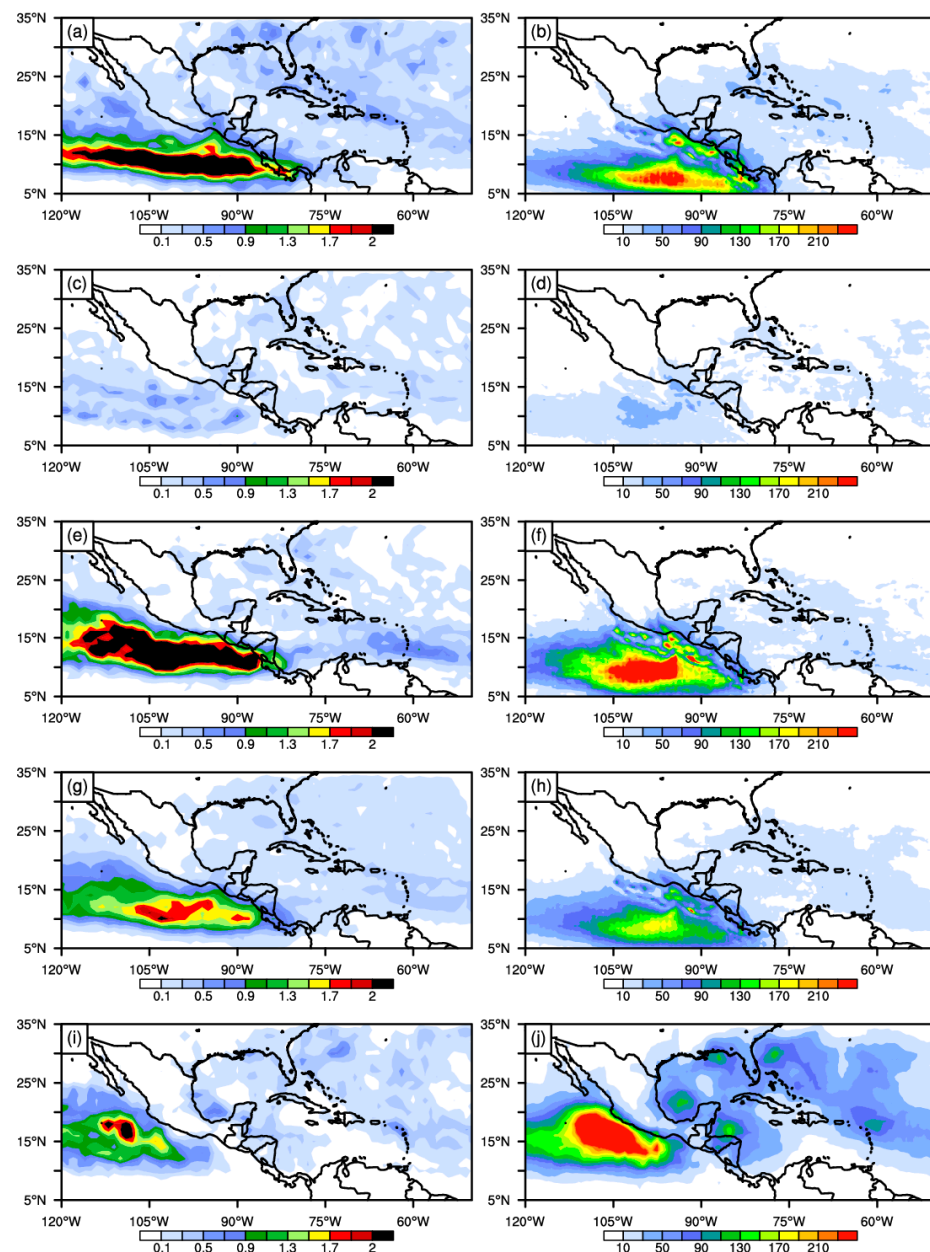


Figure 4. Mean annual tropical cyclone density for three members of the RCM ensemble: (a) rktm, (c) rnty, (e) rtty, (g) ensemble mean, (i) HURDAT, and mean annual tropical cyclone rainfall for three members of the RCM ensemble: (b) rktm, (d) rnty, (f) rtty, (h) ensemble mean, and (j) ERAI during the 1990–2000 period.

Mean annual TC-related rainfall was also computed for the 1990–2000 period using the ERAI database. In general, all members acceptably simulate TC precipitation (less than 90 mm/y) over NATL (Figure 4b,d,f). The main difference, when compared with ERAI, is located over the Gulf of Mexico, where TC rainfall is more than 110 mm/yr in some parts (Figure 4j). Over the EPAC, the members rktm and rtty produce their maximum southwards (10–15° N) of the ERAI maximum (Figure 4b,f). This overrepresentation could be related to the number of TCs that are simulated over this belt. Nevertheless, the member rnty poorly represents both TC frequency and TC-related rainfall over EPAC, which balances the ensemble mean, making it similar to observations over this basin.

Jaye et al. [62] reveal that the members rktm and rnty project a decrease in the TC frequency over NATL from the 2020–2030 period through the end of the century. Only the member rtty shows a small increase in TC activity by the 2080–2090 period. Furthermore,

Bruyère et al. [7] show that the ensemble mean also projects a 30% reduction of the TC activity over NATL and a 35% decrease over the Gulf of Mexico, which is partly consistent with Roberts et al. [15], who studied the whole NATL basin. In general, the three members project a reduction in the spatial distribution of TC tracks over the Eastern NATL but show slight spatial differences over the Gulf of Mexico for all the future decades, which are significant at a 95% confidence level (Figure 5). Moreover, the three members and the ensemble mean project significant negative changes in TC activity over EPAC during all the future decades, the most abrupt reduction being in the 105–120° W region and near the Central American coast (where TC activity is overestimated by the members rktm and rtty) by the end of the century (Figure 5). These results are consistent with Torres-Alavez et al. [8], who found a decrease in future TC activity over EPAC using the RegCM4 model driven by three CMIP5 models using RCP2.6 and RCP8.5 for making regional projections over the CORDEX domain.

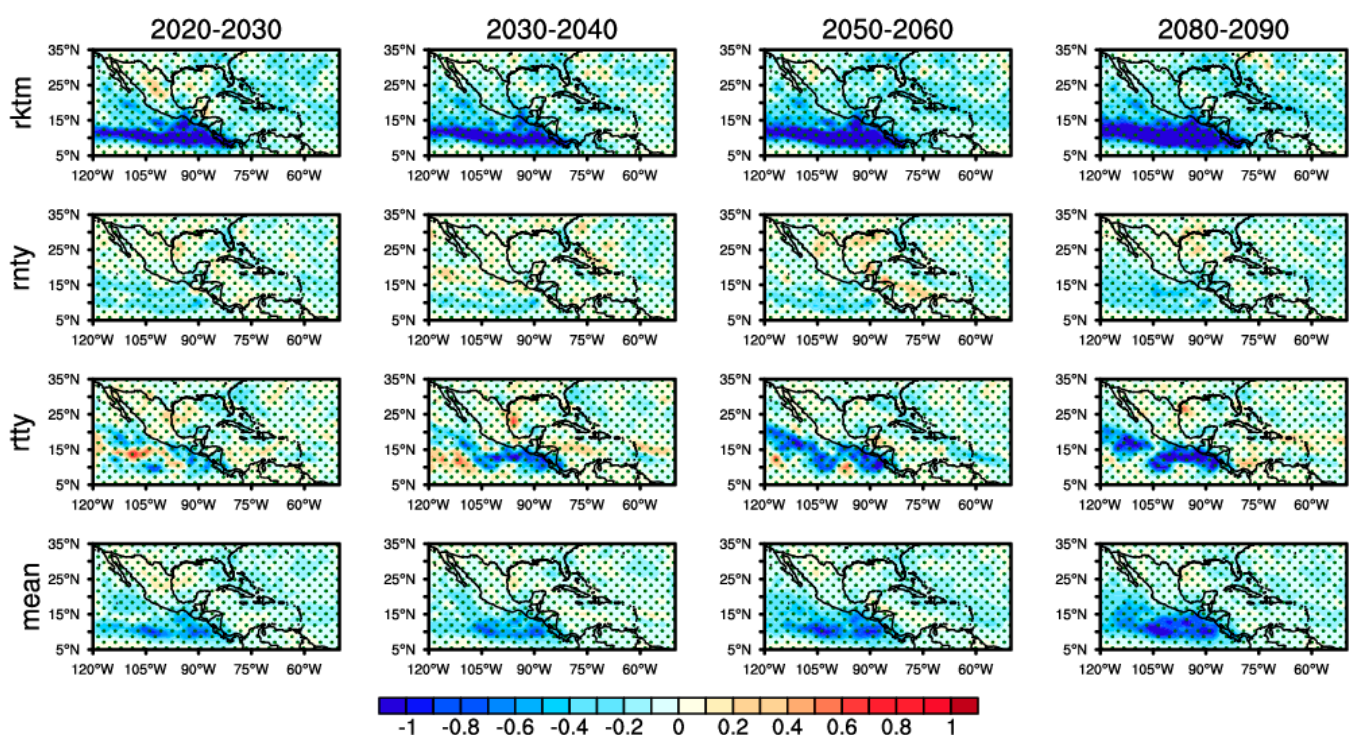


Figure 5. Annual mean anomalies of tropical cyclone density in the future ensemble runs over Tropical North America with respect to the reference period (1990–2000). The dotted regions indicate a 95% significance level applying the Kolmogorov–Smirnov two-sample test.

In terms of TC-related rainfall, Figure 6 shows that all members project a diminishment of up to 80% of the mean TC precipitation over the Caribbean region, southern Mexico, and Central America (not significant) for most decades. This reduction of TC-related rainfall partly explains the decrease in summer rainfall over Central America and the Caribbean region, as shown in Figure 3, as TCs contribute up to 15% of summer rainfall [4]. The RCM outputs have a large uncertainty over the Central American and eastern part of the EPAC, since the KST shows that the samples belong to the same distribution, and this non-significant region mainly expands the area during the last two decades.

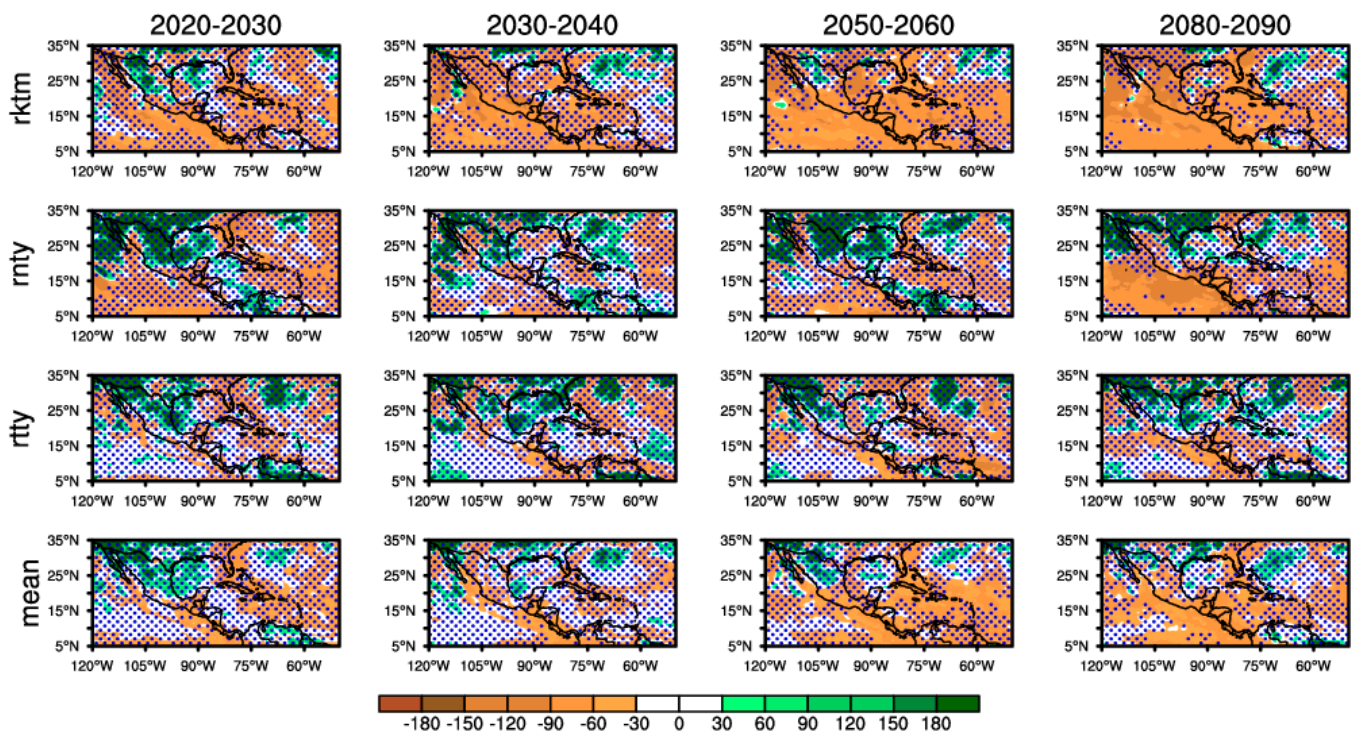


Figure 6. Mean annual percent change (%) in precipitation associated with tropical cyclones in the future ensemble runs with respect to the reference period (1990–2000). The dotted regions indicate a 95% significance level applying the Kolmogorov–Smirnov two-sample test.

A significant increase that ranges from 40% to 200% in mean annual TC precipitation over semiarid regions, as northern Mexico and the southwestern USA, is projected by the members rnty and rtty across the four future decades (Figure 6). The member rktm only projects a rise in mean annual TC precipitation for the 2020–2030 and 2050–2060 decades. In general, the ensemble mean shows a decrease in the mean annual TC precipitation for the regions mentioned above and an increase by at least 40% for northern Mexico, mainly during the 2020–2030 and 2050–2060 decades (Figure 6). These results demonstrate that the positive changes in summer rainfall over northern Mexico (Figure 3) are essentially due to an increase in TC precipitation for the members rnty and rtty during the 2020–2030 and 2050–2060 decades, as TCs represent up to 60% of the summer rainfall over semiarid Mexican regions [4]. Interestingly, these results agree with the observed positive trends in TC rainfall and TC days over northwestern Mexico found by Dominguez et al. [3] using CHIRPS during the 1981–2017 period.

3.3. Changes in Easterly Wave Features: Seasonal Precipitation, Track Density, and Tropical Cyclogenesis

Mean annual EW track densities were computed as mentioned above for TCs per unit area ($1^\circ \times 1^\circ$). Dominguez et al. [25] examined the EW activity in 10 members of the 24-member ensemble and ERAI for the 1990–2000 period. This study demonstrated that the members rktm, rnty, and rtty simulate EW activity adequately over the MDR when compared to ERAI. However, these members underestimated the maximum EW activity near the West Central American coast (see Figure 10 in Dominguez et al. [25] for further information). This underrepresentation suggests that vortices that form near this region have such strong winds that are not considered EWs because they quickly evolve to TCs.

Using the previous results provided by Dominguez et al. [25], mean annual anomalies of EW track density were calculated for future climate runs (Figure 7). Over NATL, the members rktm and rnty show significant negative anomalies of EW track density for the southern waveguide for the 2020–2030 and 2030–2040 over the MDR, but, later, the EW

activity is projected to scarcely increase by the end of the century (Figure 7). The opposite is shown for the northern waveguide. Intriguingly, the member *rtty* indicates a higher increment for the southern waveguide during the 2050–2060 and 2080–2090 decades. As a result, the ensemble mean projects a slight increase in EW activity southwards 10° N (Figure 7), which is the waveguide that provides “the seeds” for the tropical cyclogenesis that occurs over MDR [22].

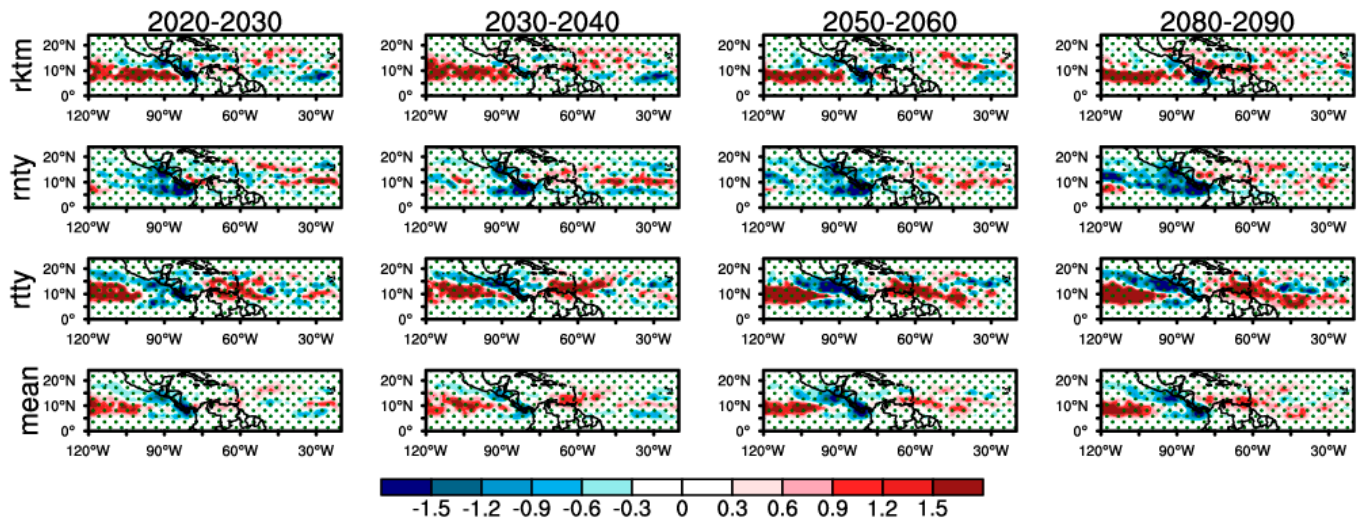


Figure 7. Mean annual anomalies of easterly wave track density in the future ensemble runs with respect to the reference period (1990–2000). The dotted regions indicate a 95% significance level applying the Kolmogorov–Smirnov two-sample test.

Over the EPAC basin, the members *rktm* and *rtty* point out a significant shift of the EW activity westwards during all the future decades, but the member *rtty* shows an opposite signal. In general, the ensemble mean indicates a decrement in EW activity over Central America (where activity is underestimated in the current climate runs) and an increment in the EW activity westwards across the future decades (Figure 7). The latter could have future implications for changes in tropical cyclogenesis locations and the type of TC track that will prevail over this basin, as TC tracks that form far away from continental landmass have a drying effect over land [4].

Dominguez et al. [25] also demonstrated that the members *rktm* and *rtty* produced dry EWs, as their associated precipitation was less than 200 mm/yr over EPAC during the 1990–2000 period. However, the rainfall is well represented by the member *rtty* over the same basin. For the MDR, the three members adequately captured the EW precipitation. Additionally, it is important to note that the three members project a reduction by up to 60% of EW rainfall for the upcoming decades, mainly over the Caribbean region, the Gulf of Mexico, central-southern Mexico, and Central America (not significant). This reduction is the principal cause for the projected decrease in summer rainfall over those regions (Figure 3), as EW contribution to summer rainfall ranges from 50% over the Caribbean region, part of the Gulf of Mexico, and central-southern Mexico, to 60% over Central America [25]. The latter region results are not significant because it seems that the RCM outputs have problems while simulating EW rainfall (Figure 8). This constraint is also shown by the results for TC rainfall over that region (Figure 6).

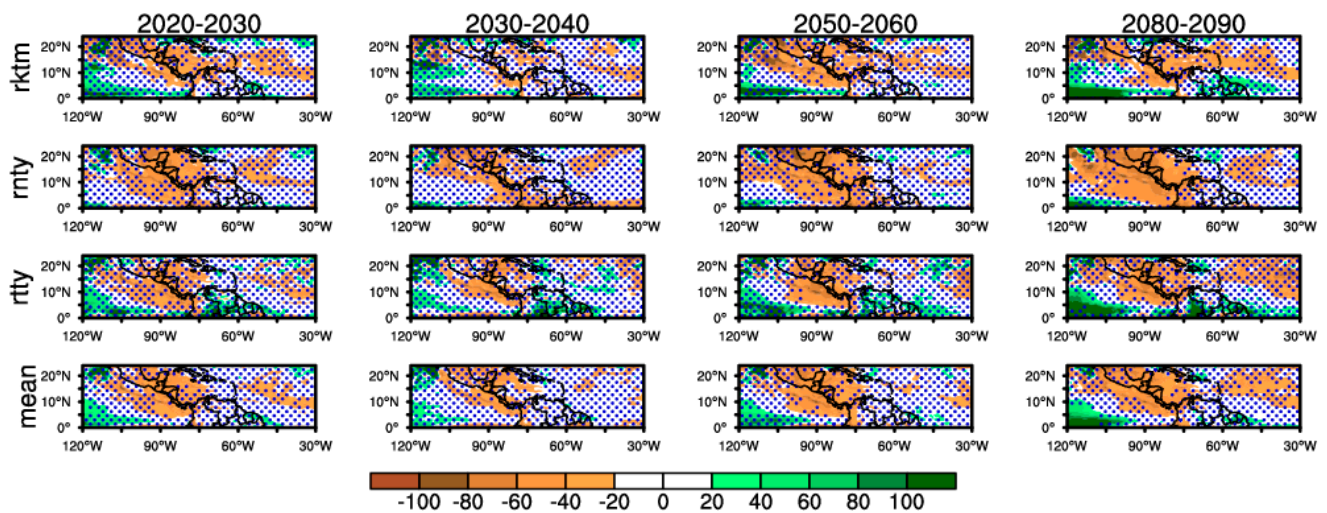


Figure 8. Mean annual percent change (%) in precipitation associated with Easterly Waves in the future ensemble runs with respect to the reference period (1990–2000). The dotted regions indicate a 95% significance level applying the Kolmogorov–Smirnov two-sample test.

In the current climate runs, the members *rktm*, *rnty*, and *rtty* overestimate the mean annual contribution of EWs to summer rainfall, which is obtained from adding all the EW-related precipitation divided by the accumulated precipitation from May to November and then multiplied by 100% to express it in terms of percentage, over the MDR [25]. However, these members tend to underestimate the contribution to summer precipitation only over Central America during the 1990–2000 period (see Figure 13 in Dominguez et al. [25]).

Interestingly, the member *rtty* shows an increase of 16% in the contribution of EWs to summer rainfall for the 2050–2060 and 2080–2090 decades, mainly over Northern South America (Figure 9). This rise is probably linked to the projected positive change in EW activity during the same decades (Figure 7). On the contrary, the ensemble mean shows a reduction by up to 8% in the contribution to summer rainfall over the Caribbean region and central-southern Mexico for all the upcoming decades (Figure 9). These results support the findings shown in Figures 3 and 8 for the same regions, which suggest that the Caribbean region and Mexico could be affected by drier EWs that could produce less precipitation over the continental landmass. The latter could have implications for regional accumulated rainfall and, consequently, water availability. Besides, the KST shows that the results from *rnty* and the ensemble mean are not robust for Central America, as future simulations seem to belong to the same distribution of the current climate runs.

Analyzing TCs that come from EWs is important, as 80% of intense hurricanes originate from EWs over NATL [63]. In this study, the percentage of TCs that come from EWs is named tropical cyclogenesis. The hurricane matching technique for the 1990–2000 period shows that 50% of TCs over NATL formed from EWs and 70% of TCs over EPAC originated from these tropical waves [25]. Additionally, Dominguez et al. [25] found that the member *rktm* simulated 28.8% and 43.9% of tropical cyclogenesis over NATL and EPAC, respectively. The member *rnty* has similar percentages, 41% and 64.2%, to those observed for the NATL and EPAC, respectively. Notwithstanding, the member *rtty* poorly captured the tropical cyclogenesis in both basins because it only detected 17.7% and 15.8% of TCs originating from EWs over NATL and EPAC, respectively [25]. In this sense, *rktm* (*rtty*) has large biases in capturing tropical cyclogenesis because the difference with the observed percentage is 21.2% (32.3%) for NATL and 26.1% (54.2%) for EPAC.

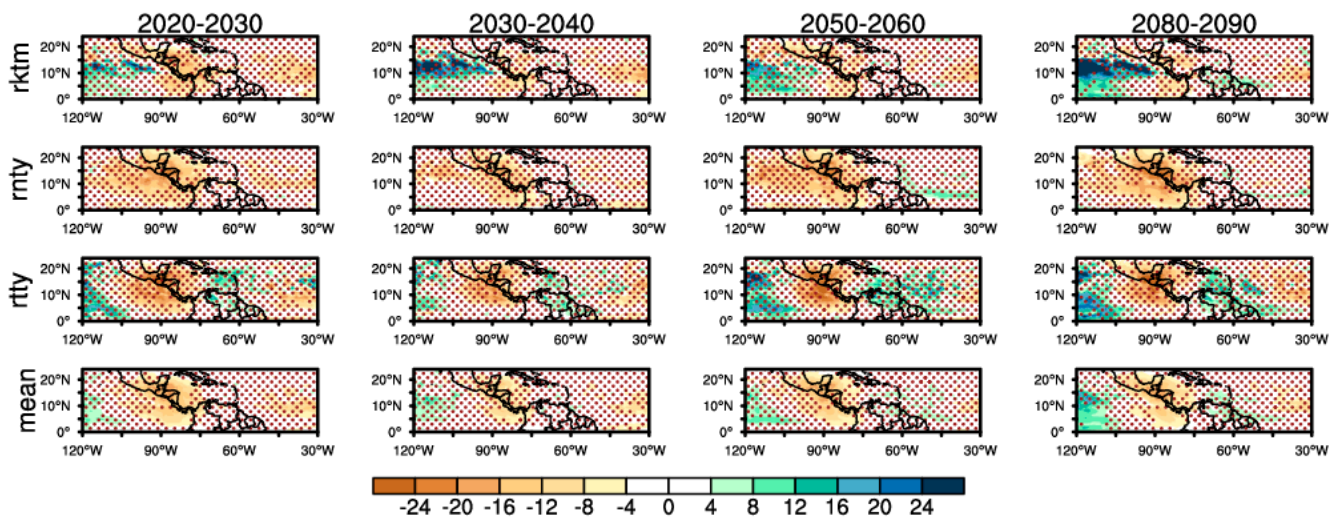


Figure 9. Mean annual percent change (%) in the contribution of Easterly Waves to summer precipitation in the future ensemble runs with respect to the reference period (1990–2000). The dotted regions indicate a 95% significance level applying the Kolmogorov–Smirnov two-sample test.

Even though most of the changes are not significant, the three members and the ensemble mean indicates a decrease by up to 9% in the number of TCs that come from EWs over NATL, except for the member *rtty* during the 2020–2030 period and for *rnty* during the 2030–2040 period (Figure 10a), whose simulated tropical cyclogenesis has large biases for the baseline period. These members indicate an increase in the southern waveguide, and further research should be carried out to understand these changes. Surprisingly, the smallest decrement in tropical cyclogenesis is projected for the 2080–2090 decade (Figure 10a). These negative changes for the upcoming decades could probably be associated with unfavorable large-scale environments for tropical cyclogenesis [62]. For the EPAC basin, most of the projected changes are not significant. Tropical cyclogenesis is projected to increase by up to 12% in the members *rktm* and *rtty* for the 2020–2030, 2030–240, and 2050–2060 decades, except for the member *rnty* during the two first decades. However, *rktm* and *rtty* have poor skill in simulating tropical cyclogenesis over EPAC. In general, the ensemble mean points out a decrease of 5% in tropical cyclogenesis over this basin during the 2080–2090 period (Figure 10b). Understanding these changes in tropical cyclogenesis using large-scale conditions over NATL and EPAC remains for future work.

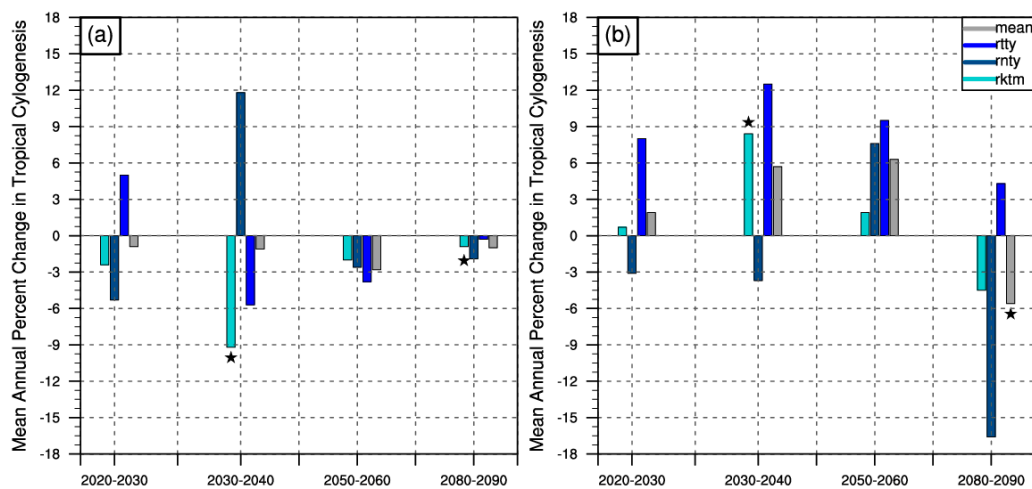


Figure 10. Mean annual percent change in tropical cyclogenesis (%) in the future ensemble runs for: (a) the North Atlantic Ocean and (b) the Eastern North Pacific Ocean with respect to the reference period (1990–2000). The stars indicate that changes have a 95% significance level applying the Kolmogorov–Smirnov two-sample test.

4. Summary and Conclusions

Tropical Cyclones (TCs) are hazardous tropical phenomena that can produce heavy rainfall and have dangerous winds, causing high economic losses [3]. However, they can also transport substantial amounts of rainfall that induce the recharge of water reservoirs, lakes, and rivers [4]. In that sense, having information about their future regional changes is crucial for decision makers in planning adaptation and mitigation strategies. Easterly Waves (EWs) are also important tropical phenomena, as they are not only precursors of TCs, but also contribute up to 60% of the seasonal rainfall (accumulated rainfall from May to November) over Tropical North America (TNA) [25].

A three-member RCM ensemble was created by NCAR, using multiple physical combinations of parameterizations for the current climate (1990–2000) using the ERAI dataset. The RCM was also driven by the Community Earth System Model (CESM) under the Representative Concentration Pathways 8.5 future emission scenario, which is the most catastrophic in terms of emission concentrations, for creating four future scenarios (2020–2030, 2030–2040, 2050–2060, 2080–2090). Biases from this global model were previously removed following Bruyère et al. [50]. The objective of having three members is to provide enough samples of different atmospheric representations. However, the three-member ensemble does not sample the full range of future possibilities linked to emission scenarios, GCM internal variability, or even different oceanic responses to radiative forcing. Our study is a first step towards looking at the meteorological mechanisms that lead to changes in tropical precipitation due to changes in EWs and TCs. To analyze these changes, we looked at individual ensemble members rather than the ensemble means.

TCs and EWs were tracked using the TRACK technique created by Hodges [51] in the current climate runs and the future climate runs of the three members (rktm, rnty, and rty). The purpose was to analyze the future changes in EW and TC features: rainfall, track density, contribution to seasonal rainfall, and tropical cyclogenesis.

Our study reveals that the three members project a reduction in the spatial distribution of TC tracks over the Eastern NATL, which is partly consistent with Roberts et al. [15], but these members show slight differences in the spatial distribution over the Gulf of Mexico for all the future decades. Moreover, the three members and the ensemble mean project significant negative changes in TC activity over EPAC during all the future decades (applying the Kolmogorov–Smirnov two-sample test), with the most abrupt reduction in the 105–120° W region and near the Central American coast, where TC activity is overestimated by the members rktm and rty by the end of the century. In terms of rainfall, while all members project a diminishment of up to 80% of the mean TC precipitation over the Caribbean region, southern Mexico, and Central America (not significant), the ensemble mean indicates an increase of at least 40% in the mean annual TC precipitation over semiarid regions, such as northern Mexico and the southwestern USA, for the four future decades.

Our analysis for future changes in EW characteristics shows that the ensemble mean projects a slight significant increase in EW activity southwards 10° N over NATL, which is the most influential waveguide for the tropical cyclogenesis that occurs over MDR. Over the EPAC basin, the ensemble mean indicates a decrease in EW activity over Central America (not significant), where the current climate runs poorly represent EW activity, and an increment in the EW activity westwards across the future decades. Future changes in EW activity could have implications for shifts in tropical cyclogenesis locations and the type of TC track that will dominate over this basin, as TC tracks that do not make landfall have a drying effect over land [4]. The ensemble mean also projects a reduction by up to 60% of EW rainfall for the upcoming decades, mainly over the Caribbean region, Gulf of Mexico, and central-southern Mexico. What is even more interesting is that these results are also supported by changes in the EW contribution to the seasonal rainfall. The ensemble mean shows a significant reduction by up to 8% in the EW contribution over the Caribbean region and central-southern Mexico for all the upcoming decades. These results suggest

that the Caribbean region and Mexico could be affected by drier EWs that could produce less precipitation over land.

The percentage of TCs that originate from EWs over NATL and EPAC (defined here as tropical cyclogenesis) is also projected to change in the upcoming decades. The ensemble mean indicates a decrease by up to 3% in the number of TCs that come from EWs over NATL during the four decades (not significant). For the EPAC basin, tropical cyclogenesis is projected to increase by up to 7% on average for the 2020–2030, 2030–2040, and 2050–2060 decades (not significant). However, the 2080–2090 decade projects a decrease of 5% on average over this basin.

The Kolmogorov–Smirnov two-sample test points out that the RCM outputs have large uncertainty mainly over Central America for the two far future decades (2050–2060 and 2080–2090). Additional RCM simulations are needed to assess if these projected changes in EW and TC features are robust using more future possible scenarios and other RCPs. Furthermore, the changes in the large-scale environments that can conduct to an increase/decrease in tropical cyclogenesis over EPAC/NATL should be further investigated. Another suggestion for future work is to compare our EW rainfall attribution technique with other techniques to provide more robustness in our results.

We conclude that future changes in tropical phenomena characteristics could significantly impact regional precipitation and, thus, future regional water availability. Their variability in the future can determine periods of droughts with high water demand or periods of enough rainfall for agricultural activities. In this sense, regional climate change scenarios should be explored, taking into account changes in the characteristics of tropical phenomena, as they can transport substantial amounts of rainfall. Additionally, future tasks should compare results from the HighResMIP ensemble with RCM outputs to gain an insightful understanding of the information provided in the regional climate change scenarios.

Author Contributions: Conceptualization, C.D.; methodology, C.D., J.M.D., and C.L.B.; validation, C.D.; formal analysis, C.D.; writing—original draft preparation, C.D., J.M.D., and C.L.B.; writing—review and editing, C.D., J.M.D., and C.L.B.; visualization, C.D. All authors have read and agreed to the published version of the manuscript.

Funding: This research received no external funding.

Data Availability Statement: The HURDAT data can be found at <https://www.nhc.noaa.gov/data/> (accessed on 13 April 2021). The ERAInterim reanalysis is available at <https://www.ecmwf.int/en/forecasts/datasets/reanalysis-datasets/era-interim> (accessed on 13 April 2021). The Reynolds optimum interpolated analysis can be found at <https://psl.noaa.gov/data/gridded/data.noaa.oisst.v2.highres.html> (accessed on 13 April 2021). The Regional Climate Outputs presented in this study are available on request. The ensemble data are not publicly available due to the fact that it was created under a contract that restricted open data repositories.

Acknowledgments: The authors are grateful to the editor and three anonymous reviewers for their helpful comments and suggestions on the early version of this manuscript. We would like to acknowledge high-performance computing support from Cheyenne provided by NCAR’s Computational and Information Systems Laboratory’s NCAR Strategic Capability allocation. NCAR is sponsored by the National Science Foundation. C.D. thanks the “Sistema Nacional de Investigadores (SNI)” from CONACyT for her fellowship.

Conflicts of Interest: The authors declare no conflict of interest.

References

1. Hsiang, S.; Camargo, S. Tropical Cyclones: From the Influence of Climate to Their Socioeconomic Impacts. In *Extreme Events: Observations, Modeling, and Economics*; Geophysical Monograph 214; John Wiley & Sons Inc.: Hoboken, NJ, USA, 2016; pp. 303–342. [[CrossRef](#)]
2. National Center for Disaster Prevention (CENAPRED). Desastres en México. 2019. Available online: <http://www.cenapred.unam.mx/es/Publicaciones/archivos/318-INFOGRAFADESASTRESENMEXICO-IMPACTOSOCIALYECONMICO.PDF> (accessed on 13 April 2021).

3. Dominguez, C.; Jaramillo, A.; Cuéllar, P. Are the Socioeconomic Impacts Associated with Tropical Cyclones in Mexico Exacerbated by Local Vulnerability and ENSO Conditions? *Int. J. Climatol.* **2021**, *41*, E3307–E3324. [[CrossRef](#)]
4. Dominguez, C.; Magaña, V. The Role of Tropical Cyclones in Precipitation Over the Tropical and Subtropical North America. *Front. Earth Sci.* **2018**, *6*, 19. [[CrossRef](#)]
5. Zhao, M.; Held, I.M. TC-Permitting GCM Simulations of Hurricane Frequency Response to Sea Surface Temperature Anomalies Projected for the Late-Twenty-First Century. *J. Clim.* **2012**, *25*, 2995–3009. [[CrossRef](#)]
6. Murakami, H.; Hsu, P.-C.; Arakawa, O.; Li, T. Influence of Model Biases on Projected Future Changes in Tropical Cyclone Frequency of Occurrence. *J. Clim.* **2014**, *27*, 2159–2181. [[CrossRef](#)]
7. Bruyère, C.L.; Rasmussen, R.; Gutmann, E.; Done, J.; Tye, M.; Jaye, A.; Prein, A.; Mooney, P.; Ge, M.; Fredrick, S.; et al. *Impact of Climate Change on Gulf of Mexico Hurricanes*; NCAR Technical Notes; National Center for Atmospheric Research: Boulder, CO, USA, 2017. [[CrossRef](#)]
8. Torres-Alavez, J.A.; Glazer, R.; Giorgi, F.; Coppola, E.; Gao, X.; Hodges, K.I.; Das, S.; Ashfaq, M.; Reale, M.; Sines, T. Future Projections in Tropical Cyclone Activity Over Multiple CORDEX Domains from RegCM4 CORDEX-CORE Simulations. *Clim. Dyn.* **2021**. [[CrossRef](#)]
9. Bacmeister, J.T.; Wehner, M.F.; Neale, R.B.; Gettelman, A.; Hannay, C.; Lauritzen, P.H.; Caron, J.M.; Truesdale, J.E. Exploratory High-Resolution Climate Simulations Using the Community Atmosphere Model (CAM). *J. Clim.* **2014**, *27*, 3073–3099. [[CrossRef](#)]
10. Wehner, M.F.; Reed, K.A.; Li, F.; Prabhat; Bacmeister, J.; Chen, C.-T.; Paciorek, C.; Gleckler, P.J.; Sperber, K.R.; Collins, W.D.; et al. The Effect of Horizontal Resolution on Simulation Quality in the Community Atmospheric Model, CAM5.1. *J. Adv. Model. Earth Syst.* **2014**, *6*, 980–997. [[CrossRef](#)]
11. Bacmeister, J.T.; Reed, K.A.; Hannay, C.; Lawrence, P.; Bates, S.; Truesdale, J.E.; Rosenbloom, N.; Levy, M. Projected Changes in Tropical Cyclone Activity under Future Warming Scenarios Using a High-Resolution Climate Model. *Clim. Chang.* **2018**, *146*, 547–560. [[CrossRef](#)]
12. Haarsma, R.J.; Roberts, M.J.; Vidale, P.L.; Senior, C.A.; Bellucci, A.; Bao, Q.; Chang, P.; Corti, S.; Fučkar, N.S.; Guemas, V.; et al. High Resolution Model Intercomparison Project (HighResMIP v1.0) for CMIP6. *Geosci. Model. Dev.* **2016**, *9*, 4185–4208. [[CrossRef](#)]
13. BAO, Q.; LIU, Y.; WU, G.; HE, B.; LI, J.; WANG, L.; WU, X.; CHEN, K.; WANG, X.; YANG, J.; et al. CAS FGOALS-F3-H and CAS FGOALS-F3-L Outputs for the High-Resolution Model Intercomparison Project Simulation of CMIP6. *Atmos. Ocean. Sci. Lett.* **2020**, *13*, 576–581. [[CrossRef](#)]
14. Roberts, M.J.; Camp, J.; Seddon, J.; Vidale, P.L.; Hodges, K.; Vanniere, B.; Mecking, J.; Haarsma, R.; Bellucci, A.; Scoccimarro, E.; et al. Impact of Model Resolution on Tropical Cyclone Simulation Using the HighResMIP-PRIMAVERA Multimodel Ensemble. *J. Clim.* **2020**, *33*, 2557–2583. [[CrossRef](#)]
15. Roberts, M.J.; Camp, J.; Seddon, J.; Vidale, P.L.; Hodges, K.; Vannière, B.; Mecking, J.; Haarsma, R.; Bellucci, A.; Scoccimarro, E.; et al. Projected Future Changes in Tropical Cyclones Using the CMIP6 HighResMIP Multimodel Ensemble. *Geophys. Res. Lett.* **2020**, *47*, e2020GL088662. [[CrossRef](#)]
16. Knutson, T.R.; Sirutis, J.J.; Vecchi, G.A.; Garner, S.; Zhao, M.; Kim, H.-S.; Bender, M.; Tuleya, R.E.; Held, I.M.; Villarini, G. Dynamical Downscaling Projections of Twenty-First-Century Atlantic Hurricane Activity: CMIP3 and CMIP5 Model-Based Scenarios. *J. Clim.* **2013**, *26*, 6591–6617. [[CrossRef](#)]
17. Knutson, T.; Camargo, S.J.; Chan, J.C.L.; Emanuel, K.; Ho, C.-H.; Kossin, J.; Mohapatra, M.; Satoh, M.; Sugi, M.; Walsh, K.; et al. Tropical Cyclones and Climate Change Assessment: Part I: Detection and Attribution. *Bull. Am. Meteorol. Soc.* **2019**, *100*, 1987–2007. [[CrossRef](#)]
18. Knutson, T.; Camargo, S.J.; Chan, J.C.L.; Emanuel, K.; Ho, C.-H.; Kossin, J.; Mohapatra, M.; Satoh, M.; Sugi, M.; Walsh, K.; et al. Tropical Cyclones and Climate Change Assessment: Part II: Projected Response to Anthropogenic Warming. *Bull. Am. Meteorol. Soc.* **2020**, *101*, E303–E322. [[CrossRef](#)]
19. Serra, Y.L.; Jiang, X.; Tian, B.; Amador-Astua, J.; Maloney, E.D.; Kiladis, G.N. Tropical Intraseasonal Modes of the Atmosphere. *Annu. Rev. Environ. Resour.* **2014**, *39*, 189–215. [[CrossRef](#)]
20. Thorncroft, C.; Hodges, K. African Easterly Wave Variability and Its Relationship to Atlantic Tropical Cyclone Activity. *J. Clim.* **2001**, *14*, 1166–1179. [[CrossRef](#)]
21. Serra, Y.L.; Kiladis, G.N.; Cronin, M.F. Horizontal and Vertical Structure of Easterly Waves in the Pacific ITCZ. *J. Atmos. Sci.* **2008**, *65*, 1266–1284. [[CrossRef](#)]
22. Chen, T.-C.; Wang, S.-Y.; Clark, A.J. North Atlantic Hurricanes Contributed by African Easterly Waves North and South of the African Easterly Jet. *J. Clim.* **2008**, *21*, 6767–6776. [[CrossRef](#)]
23. Agudelo, P.A.; Hoyos, C.D.; Curry, J.A.; Webster, P.J. Probabilistic Discrimination between Large-Scale Environments of Intensifying and Decaying African Easterly Waves. *Clim. Dyn.* **2011**, *36*, 1379–1401. [[CrossRef](#)]
24. Schreck, C.J.; Molinari, J.; Ayyer, A. A Global View of Equatorial Waves and Tropical Cyclogenesis. *Mon. Weather Rev.* **2012**, *140*, 774–788. [[CrossRef](#)]
25. Dominguez, C.; Done, J.M.; Bruyère, C.L. Easterly Wave Contributions to Seasonal Rainfall over the Tropical Americas in Observations and a Regional Climate Model. *Clim. Dyn.* **2020**, *54*, 191–209. [[CrossRef](#)]
26. Crétat, J.; Vizy, E.K.; Cook, K.H. The Relationship between African Easterly Waves and Daily Rainfall over West Africa: Observations and Regional Climate Simulations. *Clim. Dyn.* **2015**, *44*, 385–404. [[CrossRef](#)]

27. Janiga, M.A.; Thorncroft, C.D. The Influence of African Easterly Waves on Convection over Tropical Africa and the East Atlantic. *Mon. Weather Rev.* **2016**, *144*, 171–192. [[CrossRef](#)]
28. Martin, E.R.; Thorncroft, C. Representation of African Easterly Waves in CMIP5 Models. *J. Clim.* **2015**, *28*, 7702–7715. [[CrossRef](#)]
29. Kebe, I.; Diallo, I.; Sylla, M.B.; De Sales, F.; Diedhiou, A. Late 21st Century Projected Changes in the Relationship between Precipitation, African Easterly Jet, and African Easterly Waves. *Atmosphere* **2020**, *11*, 353. [[CrossRef](#)]
30. Hsieh, J.-S.; Cook, K.H. A Study of the Energetics of African Easterly Waves Using a Regional Climate Model. *J. Atmos. Sci.* **2007**, *64*, 421–440. [[CrossRef](#)]
31. Crosbie, E.; Serra, Y. Intraseasonal Modulation of Synoptic-Scale Disturbances and Tropical Cyclone Genesis in the Eastern North Pacific. *J. Clim.* **2014**, *27*, 5724–5745. [[CrossRef](#)]
32. Dee, D.P.; Uppala, S.M.; Simmons, A.J.; Berrisford, P.; Poli, P.; Kobayashi, S.; Andrae, U.; Balmaseda, M.A.; Balsamo, G.; Bauer, P.; et al. The ERA-Interim Reanalysis: Configuration and Performance of the Data Assimilation System. *Q. J. R. Meteorol. Soc.* **2011**, *137*, 553–597. [[CrossRef](#)]
33. Landsea, C.W.; Franklin, J.L. Atlantic Hurricane Database Uncertainty and Presentation of a New Database Format. *Mon. Weather Rev.* **2013**, *141*, 3576–3592. [[CrossRef](#)]
34. Jiang, H.; Zipser, E.J. Contribution of Tropical Cyclones to the Global Precipitation from Eight Seasons of TRMM Data: Regional, Seasonal, and Interannual Variations. *J. Clim.* **2010**, *23*, 1526–1543. [[CrossRef](#)]
35. Khouakhi, A.; Villarini, G.; Vecchi, G.A. Contribution of Tropical Cyclones to Rainfall at the Global Scale. *J. Clim.* **2017**, *30*, 359–372. [[CrossRef](#)]
36. Powers, J.G.; Klemp, J.B.; Skamarock, W.C.; Davis, C.A.; Dudhia, J.; Gill, D.O.; Coen, J.L.; Gochis, D.J.; Ahmadov, R.; Peckham, S.E.; et al. The Weather Research and Forecasting Model: Overview, System Efforts, and Future Directions. *Bull. Am. Meteorol. Soc.* **2017**, *98*, 1717–1737. [[CrossRef](#)]
37. Reynolds, R.W.; Smith, T.M.; Liu, C.; Chelton, D.B.; Casey, K.S.; Schlax, M.G. Daily High-Resolution-Blended Analyses for Sea Surface Temperature. *J. Clim.* **2007**, *20*, 5473–5496. [[CrossRef](#)]
38. Done, J.M.; Holland, G.J.; Bruyère, C.L.; Leung, L.R.; Suzuki-Parker, A. Modeling High-Impact Weather and Climate: Lessons from a Tropical Cyclone Perspective. *Clim. Chang.* **2015**, *129*, 381–395. [[CrossRef](#)]
39. Mlawer, E.J.; Taubman, S.J.; Brown, P.D.; Iacono, M.J.; Clough, S.A. Radiative Transfer for Inhomogeneous Atmospheres: RRTM, a Validated Correlated-k Model for the Longwave. *J. Geophys. Res. Atmos.* **1997**, *102*, 16663–16682. [[CrossRef](#)]
40. Kain, J.S.; Fritsch, J.M. A One-Dimensional Entraining/Detraining Plume Model and Its Application in Convective Parameterization. *J. Atmos. Sci.* **1990**, *47*, 2784–2802. [[CrossRef](#)]
41. Han, J.; Pan, H.-L. Revision of Convection and Vertical Diffusion Schemes in the NCEP Global Forecast System. *Weather Forecast.* **2011**, *26*, 520–533. [[CrossRef](#)]
42. Tiedtke, M. A Comprehensive Mass Flux Scheme for Cumulus Parameterization in Large-Scale Models. *Mon. Weather Rev.* **1989**, *117*, 1779–1800. [[CrossRef](#)]
43. Thompson, G.; Field, P.R.; Rasmussen, R.M.; Hall, W.D. Explicit Forecasts of Winter Precipitation Using an Improved Bulk Microphysics Scheme. Part II: Implementation of a New Snow Parameterization. *Mon. Weather Rev.* **2008**, *136*, 5095–5115. [[CrossRef](#)]
44. Janjić, Z.I. The Step-Mountain Eta Coordinate Model: Further Developments of the Convection, Viscous Sublayer, and Turbulence Closure Schemes. *Mon. Weather Rev.* **1994**, *122*, 927–945. [[CrossRef](#)]
45. Hong, S.-Y.; Noh, Y.; Dudhia, J. A New Vertical Diffusion Package with an Explicit Treatment of Entrainment Processes. *Mon. Weather Rev.* **2006**, *134*, 2318–2341. [[CrossRef](#)]
46. Chen, F.; Dudhia, J. Coupling an Advanced Land Surface–Hydrology Model with the Penn State–NCAR MM5 Modeling System. Part I: Model Implementation and Sensitivity. *Mon. Weather Rev.* **2001**, *129*, 569–585. [[CrossRef](#)]
47. Hurrell, J.W.; Holland, M.M.; Gent, P.R.; Ghan, S.; Kay, J.E.; Kushner, P.J.; Lamarque, J.-F.; Large, W.G.; Lawrence, D.; Lindsay, K.; et al. The Community Earth System Model: A Framework for Collaborative Research. *Bull. Am. Meteorol. Soc.* **2013**, *94*, 1339–1360. [[CrossRef](#)]
48. Taylor, K.E.; Stouffer, R.J.; Meehl, G.A. An Overview of CMIP5 and the Experiment Design. *Bull. Am. Meteorol. Soc.* **2012**, *93*, 485–498. [[CrossRef](#)]
49. Moss, R.H.; Nakicenovic, N.; O’Neill, B.C. Towards New Scenarios for Analysis of Emissions, Climate Change, Impacts, and Response Strategies. In Proceedings of the IPCC Expert Meeting on New Scenarios, Noordwijkerhout, The Netherlands, 19–21 September 2007; Moss, R., Intergovernmental Panel on Climate Change, Eds.; IPCC Expert Meeting Report; Intergovernmental Panel on Climate Change: Geneva, Switzerland, 2008; ISBN 978-92-9169-125-8.
50. Bruyère, C.L.; Done, J.M.; Holland, G.J.; Fredrick, S. Bias Corrections of Global Models for Regional Climate Simulations of High-Impact Weather. *Clim. Dyn.* **2014**, *43*, 1847–1856. [[CrossRef](#)]
51. Hodges, K.I. Feature Tracking on the Unit Sphere. *Mon. Weather Rev.* **1995**, *123*, 3458–3465. [[CrossRef](#)]
52. Walsh, K.J.E.; Fiorino, M.; Landsea, C.W.; McInnes, K.L. Objectively Determined Resolution-Dependent Threshold Criteria for the Detection of Tropical Cyclones in Climate Models and Reanalyses. *J. Clim.* **2007**, *20*, 2307–2314. [[CrossRef](#)]
53. Serra, Y.L.; Kiladis, G.N.; Hodges, K.I. Tracking and Mean Structure of Easterly Waves over the Intra-Americas Sea. *J. Clim.* **2010**, *23*, 4823–4840. [[CrossRef](#)]

54. Wilks, D. Statistical Methods in the Atmospheric Sciences. In *International Geophysics*, 3rd ed.; Elsevier: Amsterdam, The Netherlands; Academic Press: Boston, MA, USA, 2011; Volume 100, ISBN 978-0-12-385022-5.
55. Zhang, Y.; Fueglistaler, S. Mechanism for Increasing Tropical Rainfall Unevenness with Global Warming. *Geophys. Res. Lett.* **2019**, *46*, 14836–14843. [[CrossRef](#)]
56. Murakami, H.; Vecchi, G.A.; Underwood, S.; Delworth, T.L.; Wittenberg, A.T.; Anderson, W.G.; Chen, J.-H.; Gudgel, R.G.; Harris, L.M.; Lin, S.-J.; et al. Simulation and Prediction of Category 4 and 5 Hurricanes in the High-Resolution GFDL HiFLOR Coupled Climate Model. *J. Clim.* **2015**, *28*, 9058–9079. [[CrossRef](#)]
57. Emanuel, K. Response of Global Tropical Cyclone Activity to Increasing CO₂: Results from Downscaling CMIP6 Models. *J. Clim.* **2021**, *34*, 57–70. [[CrossRef](#)]
58. Gutmann, E.D.; Rasmussen, R.M.; Liu, C.; Ikeda, K.; Bruyere, C.L.; Done, J.M.; Garrè, L.; Friis-Hansen, P.; Veldore, V. Changes in Hurricanes from a 13-Yr Convection-Permitting Pseudo-Global Warming Simulation. *J. Clim.* **2018**, *31*, 3643–3657. [[CrossRef](#)]
59. Saha, S.; Moorthi, S.; Pan, H.-L.; Wu, X.; Wang, J.; Nadiga, S.; Tripp, P.; Kistler, R.; Woollen, J.; Behringer, D.; et al. The NCEP Climate Forecast System Reanalysis. *Bull. Am. Meteorol. Soc.* **2010**, *91*, 1015–1058. [[CrossRef](#)]
60. Durán-Quesada, A.M.; Sorí, R.; Ordoñez, P.; Gimeno, L. Climate Perspectives in the Intra-Americas Seas. *Atmosphere* **2020**, *11*, 959. [[CrossRef](#)]
61. Imbach, P.; Locatelli, B.; Zamora, J.C.; Fung, E.; Calderer, L.; Molina, L.; Ciais, P. Impacts of Climate Change on Ecosystem Hydrological Services of Central America: Water Availability. In *Climate Change Impacts on Tropical Forests in Central America: An Ecosystem Service Perspective*; Aline, C., Ed.; Routledge Publishing: New York, NY, USA, 2015; ISBN 978-0-415-72080-9.
62. Jaye, A.B.; Bruyère, C.L.; Done, J.M. Understanding Future Changes in Tropical Cyclogenesis Using Self-Organizing Maps. *Weather Clim. Extrem.* **2019**, *26*, 100235. [[CrossRef](#)]
63. Landsea, C.W. A Climatology of Intense (or Major) Atlantic Hurricanes. *Mon. Weather Rev.* **1993**, *121*, 1703–1713. [[CrossRef](#)]